On the Systematic Synthesis of OTA-Based KHN Filters

YongAn LI

School of Physics and Electronic Engineering, Xianyang Normal University, Xianyang 712000, China

lya6189@tom.com

Abstract. *According to the nullor-mirror descriptions of OTA, the NAM expansion method for three different types of KHN filters employing OTAs is considered. The type-A filters employing five OTAs have 32 different forms, the type-B filters employing four OTAs have 32 different forms, and the type-C filters employing three OTAs have eight different forms. At last a total of 72 circuits are received. Having used canonic number of components, the circuits are easy to be integrated and both pole frequency and Q-factor can be tuned electronically through tuning bias currents of the OTAs. The MULTISIM simulation results have been included to verify the workability of the derived circuit.*

Keywords

KHN filter, OTA, nullor-mirror element, nodal admittance matrix expansion.

1. Introduction

Recently, a symbolic framework for systematic synthesis of linear active circuit was presented in [1]-[6]. This method, called nodal admittance matrix (NAM) expansion, is very useful in generation of a series of novel circuits. Fortunately, the literature on current conveyor (CCII) and inverting current convey (ICC II) based gyrators [7]-[9], oscillators [10], [11] and filters [12], [13] has explained this viewpoint well. However, most of the circuits mentioned in earlier works are based on the CC II or ICC II. Very recently, it has also been found that NAM expansion method is generalized to operation transconductance amplifier (OTA) [14]-[19].

It is well known that the operational transconductance amplifier (OTA) has attracted considerable attention. A number of OTA-based filters and oscillators have been reported [20]-[26]. Unfortunately, the design methods for the circuits using OTAs are short of the systematic characteristic. For this reason, the paper aims at using NAM expansion method to realize KHN (W. J. Kerwin, L. P. Huelsman, and R. W. Newcomb) filters employing OTAs. First, according to the number of the OTA in the filters, the filters are classified as three different types. Next, the NAM expansion method for three different types of the filters is considered. The type-A filters employing five single output OTAs (SO-OTAs) have 32 different forms, the type-B filters employing four OTAs, namely four SO-OTAs or one DO-OTA and three SO-OTAs, have 32 different forms, and the type-C filters employing three OTAs, namely two DO-OTAs and one SO-OTA, have eight different forms. Having used canonic number of components, the circuits are easy to be integrated and the parameters of the filters can be tuned electronically through tuning bias currents of the OTAs. The last, the workability for one of the derived filters was verified by means of the NI MULTISIM 11.0 software. The simulation results are in agreement with theory.

2. Systematic Synthesis of KHN Filters

2.1 NAM Equation of KHN Filters

KHN filters can provide simultaneously the three basic filtering functions, namely the high-pass, band-pass and low-pass responses, at three different outputs. Fig. 1 shows a non-inverting KHN circuit using three op amps [27].

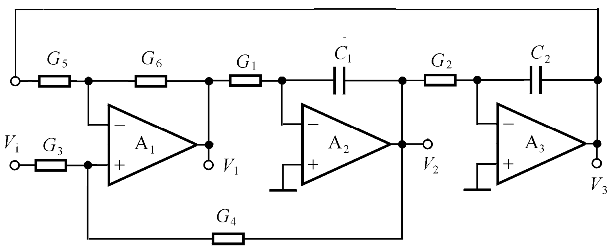

Fig. 1. A non-inverting KHN circuit using three op amps.

Taking Fig. 1 into account, and setting $V_i = 0$, $G_3 + G_4 = G_5 + G_6$, the state equations are

$$\begin{cases} sC_1V_1 + G_1V_3 = 0, \\ G_2V_1 + sC_2V_2 = 0, \\ -G_4V_1 + G_5V_2 + G_6V_3 = 0. \end{cases} \quad (1)$$

From (1) and taking the capacitors C_1 and C_2 as external elements at nodes 1 and 2, the denominator of the transfer function is given by

$$D(s) = s^2 + sG_1G_4 / C_1G_6 + G_1G_2G_5 / C_1C_2G_6 . \quad (2)$$

It follows that the pole frequency and the quality factor for the filter can be expressed by

$$f_o = \frac{1}{2\pi}\sqrt{\frac{G_1 G_2 G_5}{C_1 C_2 G_6}}\,, \tag{3}$$

$$Q = \frac{1}{G_4}\sqrt{\frac{C_1 G_2 G_5 G_6}{C_2 G_1}}\,. \tag{4}$$

From (1) the admittance matrix for the filter considered in the paper is given by

$$Y = \begin{bmatrix} sC_1 & 0 & G_1 \\ G_2 & sC_2 & 0 \\ -G_4 & G_5 & G_6 \end{bmatrix}. \tag{5a}$$

As shown in the literature [12], the port admittance matrices of the other three classes of Fig. 1 can be obtained as follows:

$$Y = \begin{bmatrix} sC_1 & 0 & -G_1 \\ -G_2 & sC_2 & 0 \\ G_4 & G_5 & G_6 \end{bmatrix}, \tag{5b}$$

$$Y = \begin{bmatrix} sC_1 & 0 & G_1 \\ -G_2 & sC_2 & 0 \\ -G_4 & -G_5 & G_6 \end{bmatrix}, \tag{5c}$$

$$Y = \begin{bmatrix} sC_1 & 0 & -G_1 \\ G_2 & sC_2 & 0 \\ G_4 & -G_5 & G_6 \end{bmatrix}. \tag{5d}$$

It can be seen that KHN filters possess four port admittance matrices, which is the basis of systematic synthesis of KHN filters.

2.2 Realization of Type A KHN Circuits

According to the number of the OTA in KHN filters, the filters considered in this paper are classified as three different types. The type A filters employ five OTAs, the type B filters employ four OTAs, and the type C filters employ three OTAs. Starting from the port admittance matrices in (5a) and taking into account the type A filters with seven nodes, the first step in the NAM expansion is to add four blank rows and columns, and then use a first nullator to link columns 3 and 7 to move G_1 to the position 1, 7, then the first norator is connected between rows 1 and 7 to move G_1 to the position 7, 7. A second nullator is connected columns 1 and 6 to move G_2 to the position 2, 6, then the second norator is connected between rows 2 and 6 to move G_2 to to the position 6, 6. A third nullator is connected columns 2 and 5 to move G_5 to the position 3, 5, then the third norator is connected rows 3 and 5 to move G_5 to the position 5, 5. At last, a fourth nullator is connected columns 1 and 4 to move -G_4 to the position 3, 4, then the first current mirror is connected rows 3 and 4 to move -G_4 to be G_4 at the position 4, 4. The NAM with the added nullor-mirror elements represented by bracket notation is shown as:

$$Y = \begin{bmatrix} sC_1 & 0 & 0 & 0 & 0 & 0 & 0 \\ 0 & sC_2 & 0 & 0 & 0 & 0 & 0 \\ 0 & 0 & G_6 & 0 & 0 & 0 & 0 \\ 0 & 0 & 0 & G_4 & 0 & 0 & 0 \\ 0 & 0 & 0 & 0 & G_5 & 0 & 0 \\ 0 & 0 & 0 & 0 & 0 & G_2 & 0 \\ 0 & 0 & 0 & 0 & 0 & 0 & G_1 \end{bmatrix}. \tag{6}$$

Here, G_6, G_4, G_5, G_2 and G_1 denote the grounded admittance at nodes 3, 4, 5, 6 and 7, respectively. It is seen that this expanded matrix contains four different pairs of pathological elements, five grounded admittance, namely G_6, G_4, G_5, G_2 and G_1.

The nullor–mirror equivalent circuit for the filters described by the NAM in (6) is shown in Fig. 2.

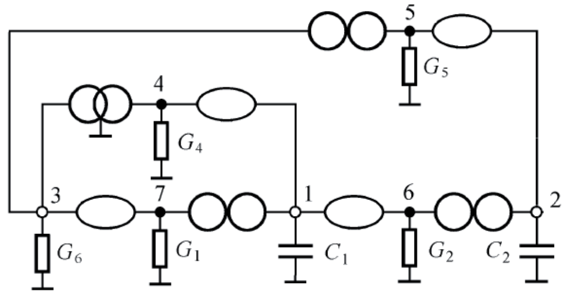

Fig. 2. Nullor-mirror equivalent circuit described by the NAM in (6).

Again, starting from the port admittance matrices in (5), and applying all possible combinations of the added nullor-mirror elements will yield 64 different forms of the expanded matrix, resulting in 64 different forms of the equivalent nullor–mirror realizations for the filter. At last, using the nullor-mirror descriptions for OTA [14-17], only 32 equivalent SO-OTA-based realizations can be achieved. Fig. 3 gives only one of 32 equivalent SO-OTA-based realizations for type-A filters. The remaining implementations is omitted to limit the paper length. Of course, readers can also obtain them by exchanging ±signs of the input and output terminals of the OTAs with the aim to provide negative feedback gains.

It should be noted that the simulation resistor using one OTA, as shown in Fig. 3, has achieved the grounded admittance, G_6 in Fig. 2.

If the non-inverting input terminal of G_6 is lifted off ground and it is driven by input V_i, the KHN filter using five SO-OTAs capable of delivering a band-pass, low–pass and high-pass outputs can be obtained, as shown in Fig. 3. The detailed analysis will be carried out in Section 3.

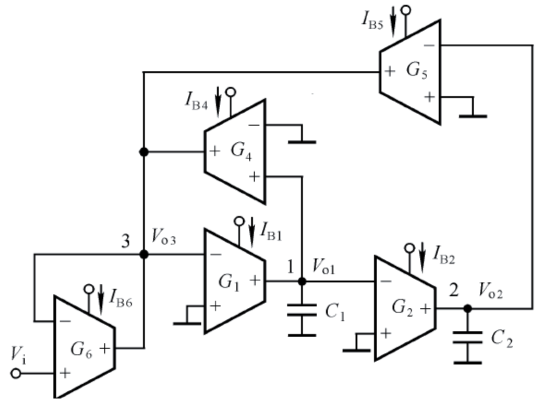

Fig. 3. One of 32 equivalent SO-OTA-based realizations for type-A filters.

2.3 Realization of Type B-class I KHN Circuits

Similarly, starting from the port admittance matrices in (5a) and setting $G_4 = G_5 = G$, following successive NAM expansion steps with the added nullor-mirror elements represented by bracket notation will yield the following expanded matrix:

$$Y = \begin{bmatrix} sC_1 & 0 & 0 & 0 & 0 & 0 & 0 \\ 0 & sC_2 & 0 & 0 & 0 & 0 & 0 \\ 0 & 0 & G_6 & 0 & 0 & 0 & 0 \\ 0 & 0 & 0 & G & -G & 0 & 0 \\ 0 & 0 & 0 & -G & G & 0 & 0 \\ 0 & 0 & 0 & 0 & 0 & G_2 & 0 \\ 0 & 0 & 0 & 0 & 0 & 0 & G_1 \end{bmatrix}. \quad (7)$$

Here, G_6, G_2 and G_1 denote the grounded admittance at nodes 3, 6 and 7, respectively. G is a floating admittance between nodes 4 and 5. It is seen that this expanded matrix contains four different pairs of pathological elements, one floating admittance, namely G, and three grounded admittance, namely G_6, G_2 and G_1

The nullor-mirror equivalent circuit for the filters described by the NAM in (7) is shown in Fig. 4.

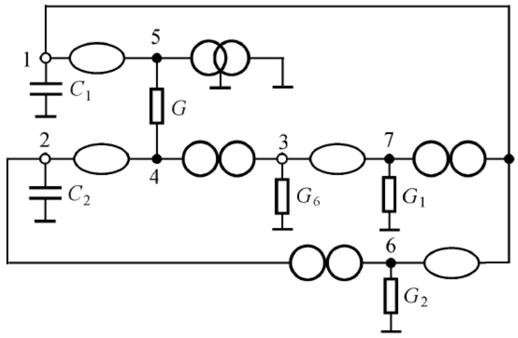

Fig. 4. Nullor-mirror equivalent circuit described by the NAM in (7).

Again, starting from the port admittance matrices in (5), and applying all possible combinations of the added nullor-mirror elements will yield 64 different forms of the expanded matrix, resulting in 64 different forms of the equivalent nullor-mirror realizations for the filters. At last, only 16 equivalent OTA-based realizations can be achieved. One is shown in Fig. 5 and the other are omitted.

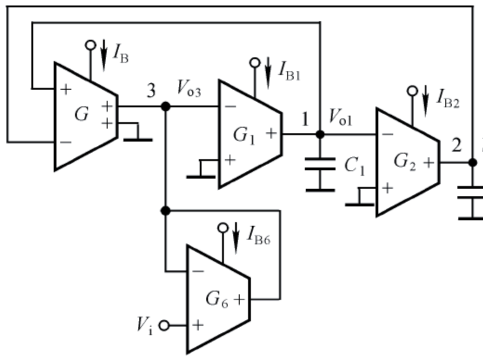

Fig. 5. One of 16 equivalent OTA-based realizations for type B-class I filters.

If the grounded terminal of G_6 is lifted off ground and it is driven by input V_i, the KHN filter using four SO-OTAs capable of delivering a band–pass, low pass and high-pass outputs can be obtained, as shown in Fig. 5.

2.4 Realization of Type B-class II KHN Circuits

Using the same manner, type B-class II filters can also be realized. Suppose $G_2 = G_4 = G$, starting from the port admittance matrices in (5a), following successive NAM expansion steps with the added nullor-mirror elements represented by bracket notation will yield the expanded matrix given by (8).

In (8), G_6, G_5 and G_1 denote the grounded admittance at nodes 3, 6 and 7, respectively. G is a floating admittance between nodes 4 and 5. It is seen that this expanded matrix contains four different pairs of pathological elements, one floating admittance, namely G, and three grounded admittance, namely G_6, G_5 and G_1.

The nullor-mirror equivalent circuit for the filters described by the NAM in (8) is shown in Fig. 6.

$$Y = \begin{bmatrix} sC_1 & 0 & 0 & 0 & 0 & 0 & 0 \\ 0 & sC_2 & 0 & 0 & 0 & 0 & 0 \\ 0 & 0 & G_6 & 0 & 0 & 0 & 0 \\ 0 & 0 & 0 & G & -G & 0 & 0 \\ 0 & 0 & 0 & -G & G & 0 & 0 \\ 0 & 0 & 0 & 0 & 0 & G_5 & 0 \\ 0 & 0 & 0 & 0 & 0 & 0 & G_1 \end{bmatrix}. \quad (8)$$

Starting from the port admittance matrices in (5), and applying all possible combinations of the added nullor-mirror elements will yield 64 different forms of the expanded matrix, resulting in 64 different forms of the equivalent nullor-mirror realizations for the filters. At last, only 16 equivalent OTA-based realizations can be achieved. One is shown in Fig. 7 and the other are omitted.

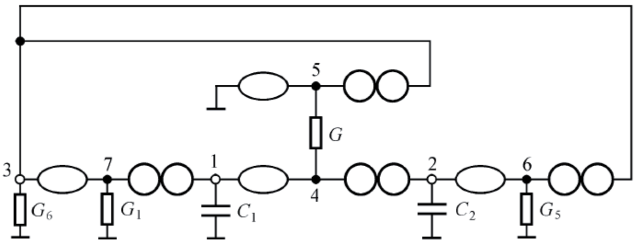

Fig. 6. Nullor-mirror equivalent circuit described by the NAM in (8).

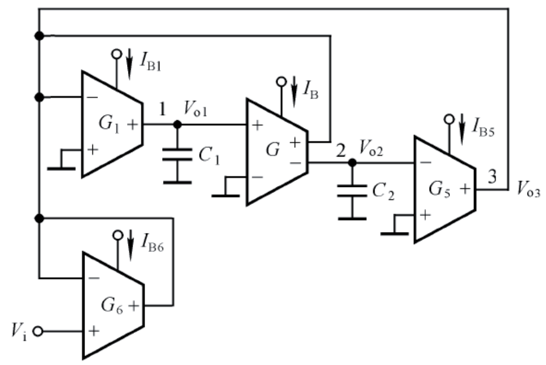

Fig. 7. One of 16 equivalent OTA-based realizations for type B-class II filters.

If the grounded terminal of G_6 is lifted off ground and it is driven by input V_i, the KHN filter using four OTAs capable of delivering a band–pass, low pass and high-pass outputs can be obtained, as shown in Fig. 7.

2.5 Realization of Type C KHN Circuits

Starting from the port admittance matrices in (5a), considering type C filters with eight nodes, the first step in the NAM expansion is to add five blank rows and columns. Then setting $G_1 = G_6$, $G_2 = G_4$, following successive NAM expansion steps with the added nullor-mirror elements represented by bracket notation will yield the following expanded matrix:

$$Y=\begin{bmatrix} sC_1 & 0 & 0 & 0 & 0 & 0 & 0 & 0 \\ 0 & sC_2 & 0 & 0 & 0 & 0 & 0 & 0 \\ 0 & 0 & 0 & 0 & 0 & 0 & 0 & 0 \\ 0 & 0 & 0 & G_2 & -G_2 & 0 & 0 & 0 \\ 0 & 0 & 0 & -G_2 & G_2 & 0 & 0 & 0 \\ 0 & 0 & 0 & 0 & 0 & G_1 & -G_1 & 0 \\ 0 & 0 & 0 & 0 & 0 & -G_1 & G_1 & 0 \\ 0 & 0 & 0 & 0 & 0 & 0 & 0 & G_5 \end{bmatrix}. \quad (9)$$

Here, G_2 is a floating admittance between nodes 4 and 5, G_1 is a floating admittance connected nodes 6 and 7, and G_5 is the admittance between node 8 and ground. It is seen that this expanded matrix contains five different pairs of pathological elements, two floating admittances, namely G_2 and G_1, and a grounded admittance, namely G_5.

The nullor-mirror equivalent circuit for the filters described by the NAM in (9) is shown in Fig. 8.

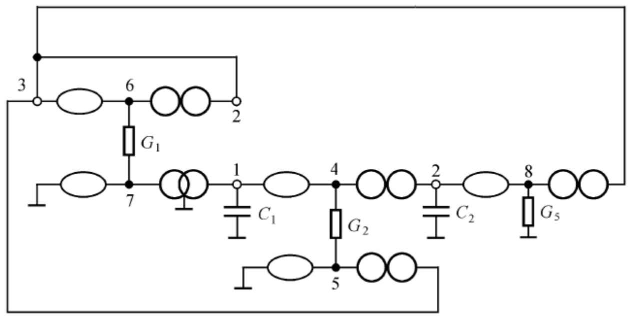

Fig. 8. Nullor-mirror equivalent circuit described by the NAM in (9).

Again, starting from the port admittance matrices in (5), and applying all possible combinations of the added nullor-mirror elements will yield 128 different forms of the expanded matrix, resulting in 128 different forms of the equivalent nullor-mirror realizations for the filters. At last, only eight equivalent OTA-based realizations can be achieved. Fig. 9 gives only one of eight equivalent OTA-based realizations for type-C filters, the remaining implementations are omitted.

If the grounded terminal of G_5 is lifted off ground and it is driven by input V_i, the OTA-based KHN filter using three OTAs capable of delivering a band–pass, low pass and high-pass outputs can be obtained, as shown in Fig. 9.

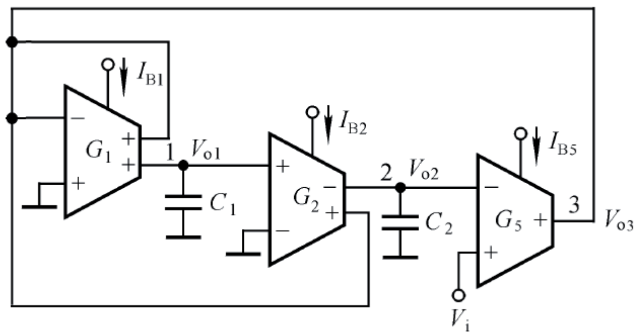

Fig. 9. One of eight equivalent OTA-based realizations for type C filters.

Although KHN filter can also be achieved by means of other methods, for example, signal-flow graph method, operation simulation method, etc, these methods lack the systematic characteristic, and one cannot obtain a series of novel circuits. Therefore, a circuit designer who understands this method well, using NAM expansion method to realize OTA-based KHN filters, has great versatility in generating new circuits.

3. Circuit Analysis

In the ideal case, for type A KHN circuits, type B-class I ones, and type B-class II ones, routine circuit analysis yields the following transfer function:

$$\frac{V_{o1}}{V_i}=\frac{-sG_1/C_1}{s^2+sG_1G_4/C_1G_6+G_1G_2G_5/C_1C_2G_6}, \quad (10a)$$

$$\frac{V_{o2}}{V_i}=\frac{G_1G_2/C_1C_2}{s^2+sG_1G_4/C_1G_6+G_1G_2G_5/C_1C_2G_6}, \quad (10b)$$

$$\frac{V_{o3}}{V_i}=\frac{s^2}{s^2+sG_1G_4/C_1G_6+G_1G_2G_5/C_1C_2G_6}. \quad (10c)$$

The pole frequency and the quality factor for the filter are the same as (3)-(4).

The corresponding band-pass, low-pass, and high-pass gains are

$$H_{BP}=-\frac{G_6}{G_4}=-\frac{I_{B6}}{I_{B4}}, \quad (11a)$$

$$H_{LP}=\frac{G_6}{G_5}=\frac{I_{B6}}{I_{B5}}, \quad (11b)$$

$$H_{HP}=1. \quad (11c)$$

For type C KHN circuits, routine circuit analysis gives the following transfer function:

$$\frac{V_{o1}}{V_i}=\frac{-sG_5/C_1}{s^2+sG_2/C_1+G_2G_5/C_1C_2}, \quad (12a)$$

$$\frac{V_{o2}}{V_i}=\frac{G_2G_5/C_1C_2}{s^2+sG_2/C_1+G_2G_5/C_1C_2}, \quad (12b)$$

$$\frac{V_{o3}}{V_i}=\frac{s^2G_5/G_1}{s^2+sG_2/C_1+G_2G_5/C_1C_2}. \quad (12c)$$

The pole frequency and the quality factor for the filter are the same as (3)-(4) with $G_1 = G_6$, $G_2 = G_4$.

The corresponding band-pass, low-pass, and high-pass gains are

$$H_{BP}=\frac{-G_5}{G_2}=\frac{-I_{B5}}{I_{B2}}, \quad (13a)$$

$$H_{LP}=1, \quad (13b)$$

$$H_{HP}=\frac{G_5}{G_1}=\frac{I_{B5}}{I_{B1}}. \quad (13c)$$

The above results have been tabulated, as shown in Tab. 1.

In the non-ideal case, to limit the paper length, only the circuit of Fig. 3 in type A filters is considered. The non-ideal effects are the tracking error of OTA, β, input parasitic capacitance C_{ip}, output parasitic capacitance C_{op}, and output parasitic conductance G_{op}. The equivalent admittance at node 3 is then

$$Y_{eq3}=G_6+G_{op4}+G_{op5}+G_{op6}+sC_{op4}+sC_{op5}+sC_{op6}+sC_{ip1}+sC_{ip6} \quad (14)$$

where $G_6 >> G_{op4}$, G_{op5}, G_{op6}, sC_{op4}, sC_{op5}, sC_{op6}, sC_{ip1}, sC_{ip}, so all the parasitic admittances at node 3 are negligible. The equivalent admittances at nodes 1 and 2 are respectively expressed as

$$Y_{eq1}=sC_1+G_{op1}+sC_{op1}+sC_{ip2}\approx s(C_1+C_{op1}+C_{ip2}),$$

$$Y_{eq2}=sC_2+G_{op2}+sC_{op2}+sC_{ip4}+sC_{ip5}\approx s(C_2+C_{op2}+C_{ip4}+C_{ip5}). \quad (15)$$

In practice, to alleviate the effects of the parasitic impedances, the tracking errors, namely β_1, β_2, β_4, β_5, β_6, and the parasitic capacitors at nodes 1 and 2, namely C_{op1}, C_{ip2}, C_{op2}, C_{ip4}, C_{ip5}, should be taken into account.

Re-analysis of the circuit in Fig. 3 yields the modified pole frequency and the quality factor:

$$f_{om}=\frac{1}{2\pi}\sqrt{\frac{\beta_1\beta_2\beta_5G_1G_2G_5}{(C_1+C_{op1}+C_{ip2})(C_2+C_{op2}+C_{ip4}+C_{ip5})\beta_6G_6}}, \quad (16)$$

$$Q_m=\frac{1}{\beta_4G_4}\sqrt{\frac{(C_1+C_{op1}+C_{ip2})\beta_2\beta_5\beta_6G_2G_5G_6}{(C_2+C_{op2}+C_{ip4}+C_{ip5})\beta_1G_1}}, \quad (17)$$

$$G_i=\frac{G_{0i}}{\sqrt{1+(\omega/\omega_{pi})^2}},\ G_{i0}=\frac{I_{B0i}}{2V_T}. \quad (18)$$

Here, $I = 1, 2, 4, 5, 6$, β_i is the tracking errors for the i^{th} OTA, G_{0i} is the zero-frequency tranconductance gain, ω_{pi} is parasitic pole frequency [28], [29], I_{B0i} is the bias current, and V_T is the thermal voltage. Assuming $\beta_1 = \beta_2 = \beta_4 = \beta_5 = \beta_6$, ignoring the second-order infinitesimal, and using $(1+x)^{0.5} \approx 1 + x/2$, for $|x| << 1$, (16)-(17) becomes

$$f_{om}=f_o\left(1-\frac{C_{op1}+C_{ip2}}{2C_1}-\frac{C_{op2}+C_{ip4}+C_{ip5}}{2C_2}\right), \quad (19)$$

$$Q_m=Q\left(1+\frac{C_{op1}+C_{ip2}}{2C_1}-\frac{C_{op2}+C_{ip4}+C_{ip5}}{2C_2}\right). \quad (20)$$

From (16)-(17), the sensitivities of f_{om} and Q_m to the passive components and tracking errors are calculated as

$$S_{\beta_1}^{f_{om}}=S_{\beta_2}^{f_{om}}=S_{\beta_5}^{f_{om}}=-S_{\beta_6}^{f_{om}}=0.5,$$

$$S_{\beta_2}^{Q_m}=S_{\beta_5}^{Q_m}=S_{\beta_6}^{Q_m}=-S_{\beta_1}^{Q_m}=0.5,\ S_{\beta_4}^{Q_m}=-1,$$

$$S_{C_1}^{f_{om}}=-S_{C_1}^{Q_m}=-\frac{1}{2[1+(C_{op1}+C_{ip2})/C_1]},$$

$$S_{C_2}^{f_{om}} = S_{C_2}^{Q_m} = -\frac{1}{2[1+(C_{op2}+C_{ip4}+C_{ip5})/C_2]},$$

$$S_{C_{op1}}^{f_{om}} = -S_{C_{op1}}^{Q_m} = -\frac{C_{op1}}{2(C_1+C_{op1}+C_{ip2})},$$

$$S_{C_{ip2}}^{f_{om}} = -S_{C_{ip2}}^{Q_m} = -\frac{C_{ip2}}{2(C_1+C_{op1}+C_{ip2})},$$

$$S_{C_{op2}}^{f_{om}} = S_{C_{op2}}^{Q_m} = -\frac{C_{op2}}{2(C_2+C_{op2}+C_{ip4}+C_{ip5})},$$

$$S_{C_{ip4}}^{f_{om}} = S_{C_{ip4}}^{Q_m} = -\frac{C_{ip4}}{2(C_2+C_{op2}+C_{ip4}+C_{ip5})},$$

$$S_{C_{ip5}}^{f_{om}} = S_{C_{ip5}}^{Q_m} = -\frac{C_{ip5}}{2(C_2+C_{op2}+C_{ip4}+C_{ip5})}. \quad (21)$$

From (16)-(18), the sensitivities of f_{om} and Q_m to the bias currents and the parasitic pole frequencies can also be calculated as

$$S_{I_{B01}}^{f_{om}} = S_{I_{B02}}^{f_{om}} = S_{I_{B05}}^{f_{om}} = -S_{I_{B06}}^{f_{om}} = 0.5,$$

$$S_{\omega_{pi}}^{f_{om}} = \frac{-0.5\omega^2}{\omega^2+\omega_{pi}^2},\ i = 1,\ 2,\ 5,$$

$$S_{\omega_{p6}}^{f_{om}} = \frac{0.5\omega^2}{\omega^2+\omega_{p6}^2},$$

$$S_{I_{B02}}^{Q_m} = S_{I_{B05}}^{Q_m} = S_{I_{B06}}^{Q_m} = -S_{I_{B01}}^{Q_m} = 0.5,\ S_{I_{B04}}^{Q_m} = -1,$$

$$S_{\omega_{pi}}^{Q_m} = \frac{-0.5\omega^2}{\omega^2+\omega_{pi}^2},\ i = 2,\ 5,\ 6,$$

$$S_{\omega_{p6}}^{Q_m} = \frac{\omega^2}{\omega^2+\omega_{p4}^2}. \quad (22)$$

From the above expressions, it is seen that all passive and active sensitivities of the circuit are low. It is also seen that the sensitivities of the pole frequency and the quality factor to the parasitic pole frequencies depend upon the frequency and will increase with frequency in magnitude, as simulated in the next section.

Class	Pass gain H	f_o and Q	Number of OTAs	Initial conditions
A	$H_{BP} = -\frac{I_{B6}}{I_{B4}}$ $H_{LP} = \frac{I_{B6}}{I_{B5}}$ $H_{HP} = 1$	$f_o = \frac{1}{4\pi V_T}\sqrt{\frac{I_{B1}I_{B2}I_{B5}}{C_1C_2I_{B6}}}$ $Q = \frac{1}{I_{B4}}\sqrt{\frac{C_1I_{B2}I_{B5}I_{B6}}{C_2I_{B1}}}$	5	No
B, I	$H_{BP} = -\frac{I_{B6}}{I_B}$ $H_{LP} = \frac{I_{B6}}{I_B}$ $H_{HP} = 1$	$f_o = \frac{1}{4\pi V_T}\sqrt{\frac{I_{B1}I_{B2}I_B}{C_1C_2I_{B6}}}$ $Q = \sqrt{\frac{C_1I_{B2}I_{B6}}{C_2I_{B1}I_B}}$	4	$G_4=G_5=G$
B, II	$H_{BP} = -\frac{I_{B6}}{I_B}$ $H_{LP} = \frac{I_{B6}}{I_{B5}}$ $H_{HP} = 1$	$f_o = \frac{1}{4\pi V_T}\sqrt{\frac{I_{B1}I_BI_{B5}}{C_1C_2I_{B6}}}$ $Q = \sqrt{\frac{C_1I_{B5}I_{B6}}{C_2I_{B1}I_B}}$	4	$G_2=G_4=G$
C	$H_{BP} = \frac{-I_{B5}}{I_{B2}}$ $H_{LP} = 1$ $H_{HP} = \frac{I_{B5}}{I_{B1}}$	$f_o = \frac{1}{4\pi V_T}\sqrt{\frac{I_{B2}I_{B5}}{C_1C_2}}$ $Q = \sqrt{\frac{C_1I_{B5}}{C_2I_{B2}}}$	3	$G_6=G_1$ $G_4=G_2$

Tab. 1. Properties of the three different types of KHN filters.

Although the input terminals of the derived filters possess high input impedance, the output terminals are not low. Therefore, these filters may not directly cascade with the other circuit blocks; it is a typical property of the OTA-based circuits using a voltage as output signal. However, if G_1, G_2, and G_5 in Fig. 3 are replaced by balance output OTAs (BO-OTA), respectively, the corresponding inverting current outputs with high output impedances, I_{o3}, I_{o1}, and I_{o2}, are then high-pass, band-pass, low-pass outputs, respectively. Hence, the cascadable connection of the former voltage-mode stage and the latter current-mode stage can be realized.

4. Simulation Results

As an example of KHN filters synthesis using OTAs, consider the circuit of Fig. 3 in type A filters. From $G_m = I_B/2V_T$ and (3)-(4), assuming $G_5 = G_6 = G$, $G_1 = G_2 = G_0$ and $C_1 = C_2 = C$. The pole frequency and the quality factor for the filter can be expressed by

$$f_o = \frac{G_0}{2\pi C} = \frac{I_{B0}}{4\pi V_T C}, \tag{23}$$

$$Q = \frac{G}{G_4} = \frac{I_B}{I_{B4}}. \tag{24}$$

Here, I_{B0} is the bias current of either G_1 or G_2, I_B is the bias current of either G_5 or G_6, and I_{B4} is the bias current of G_4.

Equation (23) shows that adjusting I_{B0} can electronically turn the pole frequency, whereas equation (24) indicates that trimming I_B can adjust the quality factor without affecting the pole frequency. This means that the circuit provides the attractive feature of independent linear current control of the pole frequency and the quality factor.

In order to test the performances of the derived circuits, the SO-OTAs of Fig. 3 employed LM13600 of the analog device library from NI MULTISIM 11.0 software, and then Fig. 3 was created. Finally, Fig. 3 circuit was simulated with ±10 V power supplies. If $C = 1$ nF, $I_{B0} = 104$ µA, $I_B = I_{B4} = 104$ µA. (This can be achieved by means of the multi-transistor current mirror [30], [31]), from (23)-(24), the design value for f_o is 318.3 kHz, the design value for Q is 1. The simulation result is shown in Fig. 10. Using the pointer in MULTISIM yields the actual values for f_o is 317.8 kHz, the actual values for Q is 0.999, the corresponding deviation is -0.16% and -0.04%, respectively.

To illustrate the controllability of the pole frequency by adjusting I_{B0}, the bias currents I_B and I_{B4} are kept to be 416 µA and 104 µA, respectively. When $I_{B0} = 104$ µA, 208 µA, and 416 µA, from (23)-(24), the design value for f_o is 318.3 kHz, 636.6 kHz, and 1.273 MHz; the design value for Q is 4. The simulation result is shown in Fig. 11. Using the pointer in MULTISIM yields the actual values for f_o is 317.8 kHz, 631.0 kHz, 1.250 MHz, the corresponding deviation is -0.16%, -0.88%, and -1.81%, respectively.

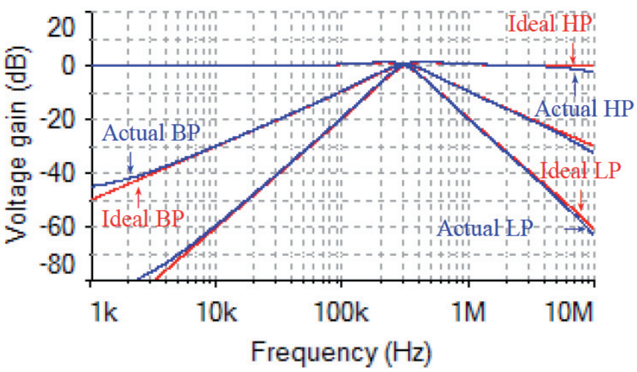

Fig. 10. Simulated characteristics of KHN filter when $C = 1$ nF, $I_{B0} = I_B = I_{B4} = 104$ µA.

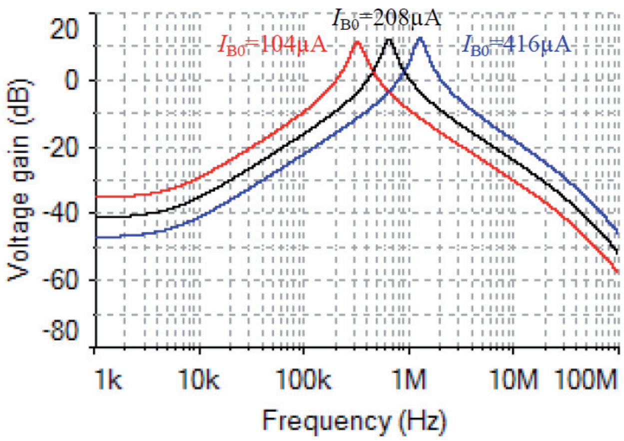

Fig. 11. Simulated characteristics of band-pass filter when $C = 1$ nF, $I_{B4} = 104$ µA, $I_B = 416$ µA, $I_{B0} = 104$ µA, 208 µA, and 416 µA.

To illustrate the controllability of the quality factor by adjusting I_B, the bias currents I_{B0} and I_{B4} are kept to be 104 µA. When $I_B = 104$ µA, 208 µA, and 416 µA, from (24), the design value for Q is 1, 2, and 4. The simulation result is shown in Fig. 12. Using the pointer in MULTISIM yields the actual values for Q of 1.02, 1.98, 3.68, the corresponding deviation is 2%, -1%, and -8%, respectively.

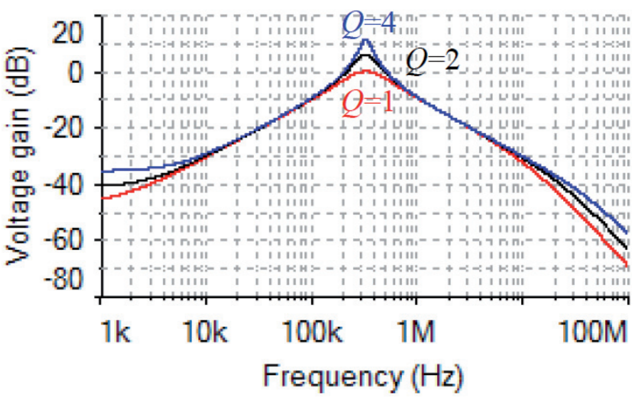

Fig. 12. Simulated characteristics of band-pass filter when $C = 1$ nF, $I_{B0} = I_{B4} = 104$ µA, $I_B = 104$ µA, 208 µA, and 416 µA.

It is obvious that the simulated results show the influence of parasitic transfer zero for high frequency band and cut-down of Q factor for value up c.3.

The time-domain response of the circuit of Fig. 3, when $C = 1$ nF, $I_{B0} = I_B = I_{B4} = 104$ µA, is shown in Fig. 13. After a sine wave of 1 mV amplitude and 318 kHz is applied as the input to the circuit, the steady-state amplitude at the node 1 is 1 mV, and the phase shift is 183^0. Fig. 14 shows the time-domain response when $V_{ip} = 1$ mV, $f = 3.18$ MHz. The steady-state amplitude at the node 1 is 98 µV, and phase shift is 90^0, which is in correspondence with the theoretical values.

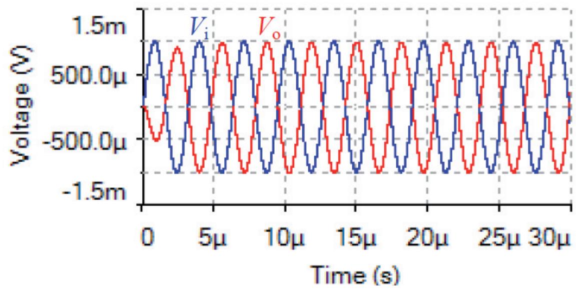

Fig. 13. Band-pass waveforms for Fig. 3 with $V_{ip} = 1$ mV, $f = 318$ kHz.

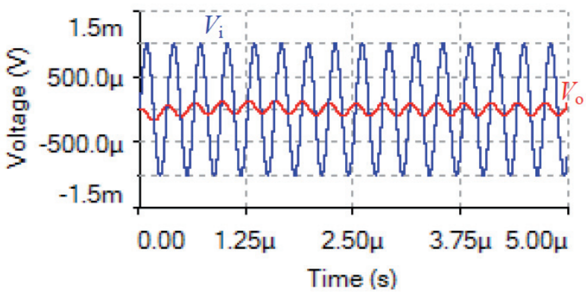

Fig. 14. Band-pass waveforms for Fig. 3 with $V_{ip} = 1$ mV, $f = 3.18$ MHz.

It is seen that MULTISIM simulation results have verified the theoretical results.

5. Conclusions

The OTA-based KHN filters given in the paper have been synthesized by using NAM expansion method. Although the CCII-based KHN filters have been realized by using NAM expansion [13], the circuits employed CCII s, rather than OTAs, cannot be tuned electronically. Consequently, this is the first paper in which the NAM expansion method is first used to synthesize KHN filters employing OTAs. The main feature of the paper is making use of systematic design method to obtain all novel KHN filters using OTAs. In addition, the derived filter enjoys the following features:

- Current control of the pole frequency and the quality factor by adjusting the bias currents of OTAs;
- Use of grounded capacitors;
- No externally connected resistors.

The results of circuit simulations are in agreement with theory.

Acknowledgement

This work is supported by the Natural Science Foundation of Shaanxi Province (Grant No. 2012JM8017) and the Scientific Research Program Funded by Shaanxi Provincial Education Department, China (Program No. 12JK0496). The author would also like to thank the anonymous reviewers for their suggestions.

References

[1] HAIGH, D. G., CLARKE, T. J. W., RADMORE, P. M. Symbolic framework for linear active circuits based on port equivalence using limit variables. *IEEE Transactions on Circuits and Systems I,* 2006, vol. 53, no. 9, p. 2011-2024.

[2] HAIGH, D. G. A method of transformation from symbolic transfer function to active-RC circuit by admittance matrix expansion. *IEEE Transactions on Circuits and Systems I,* 2006, vol. 53, no. 12, p. 2715-2728.

[3] HAIGH, D. G., RADMORE, P. M. Systematic synthesis of active–RC circuit building-blocks. *Analog Integrated Circuits and Signal Processing*, 2005, vol. 43, no. 3, p. 297-315.

[4] HAIGH, D. G., RADMORE, P. M. Admittance matrix models for the nullor using limit variables and their application to circuit design. *IEEE Transactions on Circuits and Systems I*, 2006, vol. 53, no. 10, p. 2214-2223.

[5] SOLIMAN, A. M. Transformation of oscillators using op amps, unity gain cells and CFOA. *Analog Integrated Circuits and Signal Processing*, 2010, vol. 65, p. 105-114.

[6] SOLIMAN, A. M., SAAD, R. A. The voltage mirror-current mirror pair as a universal element. *International Journal of Circuit Theory and Applications*, 2010, vol. 38, no. 8, p. 787-795.

[7] SAAD, R. A., SOLIMAN, A. M. Use of mirror elements in the active device synthesis by admittance matrix expansion. *IEEE Transactions on Circuits and Systems I*, 2008, vol. 55, no. 9, p. 2726-2735.

[8] SAAD, R. A., SOLIMAN, A. M. Generation, modeling, and analysis of CCII-based gyrators using the generalized symbolic framework for linear active circuits. *International Journal of Circuit Theory and Applications*, 2008, vol. 36, no. 3, p. 289-309.

[9] SAAD, R. A., SOLIMAN, A. M. On the systematic synthesis of CCII-based floating simulators. *International Journal of Circuit Theory and Applications*, 2010, vol. 38, no. 9, p. 935-967.

[10] SOLIMAN, A. M. Generation of current conveyor based oscillators using nodal admittance matrix expansion. *Analog Integrated Circuits and Signal Processing*, 2010, vol. 65, no.1, p. 43-59.

[11] SOLIMAN, A. M. Generation of CCII and ICCII based Wien oscillators using nodal admittance matrix expansion. *AEÜ–International Journal of Electronics and Communications*, 2010, vol. 64, no. 10, p. 971-977.

[12] SOLIMAN, A. M. Generation of Kerwin-Huelsman-Newcomb biquad filter circuits using nodal admittance expansion. *International Journal of Circuit Theory and Applications*, 2011, vol. 39, no. 7, p. 697-717.

[13] SOLIMAN, A. M. History and progress of the Tow Thomas bi-quadratic filter part III: Generation using NAM expansion. *Journal of Circuits Systems and Computers*, 2010, vol. 19, no. 3, p. 529 to 548.

[14] LI, Y. A. NAM expansion method for systematic synthesis of OTA-based floating gyrators. *AEÜ–International Journal of Electronics and Communications*, 2013, vol. 67, no. 4, p. 289-294.

[15] SOLIMAN, A. M. Tranconductance amplifiers: NAM realizations and applications, chapter 4. In: *Analog Circuits: Applications, Design and Performance*. New York: Hauppauge, Nova Science Publisher, 2012, p. 93-119.

[16] SOLIMAN, A. M. Classification and pathological realizations of transconductance amplifiers. *Journal of Circuits Systems and Computers*, 2012, vol. 21, no. 1, p. 1-17. http://dx.doi.org/10.1142/S0218126612500107.

[17] SOLIMAN, A. M. Three port gyrator circuits using transconductance amplifiers or generalized conveyors. *AEÜ-International Journal Electronics and Communication*, 2012, vol. 66, no. 4, p. 286-293.

[18] LI, Y. A. Systematic synthesis of OTA-based T-T filters using NAME method. *Journal of Circuits Systems and Computers*, 2013, vol. 22, no. 3, p. 1-17, http://dx.doi.org/10.1142/S0218126613500023.

[19] LI, Y. A. On the systematic synthesis of OTA-based Wien oscillators. *AEÜ–International Journal of Electronics and Communications*, 2013, vol. 67, no. 9, p. 754-760.

[20] BARTHELEMY, H., MEILLERE, S., GAAUBERT, J., DEHAESE, N., BOURAEL, S. OTA based on CMOS inverters and application in the design of tunable bandpass filter. *Analog Integrated Circuits and Signal Processing*, 2008, vol. 57, no. 3, p. 169-178.

[21] WANG, C. H., ZHOU. L., LI, T. A new OTA-C current-mode biquad filter with single input and multiple outputs. *AEÜ–International Journal of Electronics and Communications*, 2008, vol. 62, no. 3, p. 232-234.

[22] KUMNGERN, M., KNOBNOB, B., DEJHAN, K. Electronically tunable high–input impedance voltage-mode universal biquadratic filter based on simple CMOS OTAs. *AEÜ–International Journal of Electronics and Communications*, 2010, vol. 64, no. 10, p. 934 to 939.

[23] CHIEN, H. C., LO, Y. K. OTA-based monostable multivibrators with current tuning properties. *Microelectronics Journal*, 2011, vol. 42, no. 1, p. 188-195.

[24] LO, Y. K., CHIEN, H. C. Current-controllable monostable multivibrator with retriggerable function. *Microelectronics Journal*, 2009, vol. 40, no. 8, p. 1184-1191.

[25] RIEWRUJA, V., PETCHMANEELUMKA, W. Floating current-controlled resistance converters using OTAs. *AEÜ–International Journal of Electronics and Communications*, 2008, vol. 62, no. 10, p. 725-731.

[26] ACAR, C., ANDAY, F., KUNTMAN, H. On the realization of OTA-C filters. *International Journal of Circuit Theory and Applications*, 1993, vol. 21, no. 2, p. 331-341.

[27] SOLIMAN, A. M. Generation and classification of Kerwin-Huelsman-Newcomb circuits using the DVCC. *International Journal of Circuit Theory and Applications*, 2008, vol. 37, no. 7, p. 835-855.

[28] METIN, B., PAL, K., MINAEI, S., CICEKOGLU, O. Trade-offs in the OTA-based analog filter design. *Analog Integrated Circuits and Signal Processing*, 2009, vol. 60, no. 3, p. 205-213.

[29] PETERSON, K. D., NEDUNGADI, A., GEIGER, R. L. Amplifier design consideration for high frequency monolithic filters. In *Proc. ECCTD*, Paris (France), 1987, p. 321-326.

[30] LI, Y. A. Electronically tunable current-mode quadrature oscillator using single MCDTA. *Radioengineering*, 2010, vol. 19, no. 4, p. 667-671.

[31] LI, Y. A. Current-mode sixth-order elliptic band-pass filter using MCDTAs. *Radioengineering*, 2011, vol. 20, no. 3, p. 645-649.

About Author ...

YongAn LI was born in 1961, received BS from the Northwestern University (in China) in 1983. He is currently a professor at the School of Physics and Electronic Engineering, Xianyang Normal University, China, and is studying on analog signal processing circuits and current-mode circuits. He has authored several international journal papers and has acted as a reviewer for several international journals.